



Dalton
Transactions

**Mechanochemical Synthesis and Structural Analysis of
Trivalent Lanthanide and Uranium
Diphenylphosphinodiboranates**

Journal:	<i>Dalton Transactions</i>
Manuscript ID	DT-ART-06-2021-001932.R1
Article Type:	Paper
Date Submitted by the Author:	14-Jul-2021
Complete List of Authors:	Fetrow, Taylor; The University of Iowa, Chemistry Daly, Scott; The University of Iowa, Chemistry

SCHOLARONE™
Manuscripts

Mechanochemical Synthesis and Structural Analysis of Trivalent Lanthanide and Uranium Diphenylphosphinodiboranates

Taylor V. Fetrow and Scott R. Daly*

Department of Chemistry, The University of Iowa, E331 Chemistry Building, Iowa City, Iowa
52242, United States

Corresponding email: scott-daly@uiowa.edu

Abstract

Phosphinodiboranates ($\text{H}_3\text{BPR}_2\text{BH}_3^-$) are a class of borohydrides that have merited a reputation as weakly coordinating anions, which is attributed in part to the dearth of coordination complexes known with transition metals, lanthanides, and actinides. We recently reported how $\text{K}(\text{H}_3\text{BP}^t\text{Bu}_2\text{BH}_3)$ exhibits sluggish salt elimination reactivity with f-metal halides in organic solvents such as Et_2O and THF. Here we report how this reactivity appears to be further attenuated in solution when the $t\text{Bu}$ groups attached to phosphorus are exchanged for $\text{R} = \text{Ph}$ or H and describe how mechanochemistry was used to overcome limited solution reactivity with $\text{K}(\text{H}_3\text{BPPH}_2\text{BH}_3)$. Grinding three equivalents of $\text{K}(\text{H}_3\text{BPPH}_2\text{BH}_3)$ with $\text{UI}_3(\text{THF})_4$ or LnI_3 ($\text{Ln} = \text{Ce}, \text{Pr}, \text{Nd}$) allowed homoleptic complexes with the empirical formulas $\text{U}(\text{H}_3\text{BPPH}_2\text{BH}_3)_3$ (**1**), $\text{Ce}(\text{H}_3\text{BPPH}_2\text{BH}_3)_3$ (**2**), $\text{Pr}(\text{H}_3\text{BPPH}_2\text{BH}_3)_3$ (**3**), and $\text{Nd}(\text{H}_3\text{BPPH}_2\text{BH}_3)_3$ (**4**) to be prepared and subsequently crystallized in good yields (50-80%). Single-crystal XRD studies revealed that all four complexes exist as dimers or polymers in the solid-state, whereas ^1H and ^{11}B NMR spectra showed that they exist as a mixture of monomers and dimers in solution. Treating **4** with THF breaks up the dimer to yield the monomeric complex $\text{Nd}(\text{H}_3\text{BPPH}_2\text{BH}_3)_3(\text{THF})_3$ (**4-THF**). XRD studies revealed that **4-THF** has one chelating and two dangling $\text{H}_3\text{BPPH}_2\text{BH}_3^-$ ligands bound to the metal to accommodate binding of THF. In contrast to the results with $\text{K}(\text{H}_3\text{BPPH}_2\text{BH}_3)$, attempting the same mechanochemical reactions with the simplest phosphinodiboranate, $\text{K}(\text{H}_3\text{BPH}_2\text{BH}_3)$ were unsuccessful; only the partial metathesis product $\text{U}(\text{H}_3\text{BPH}_2\text{BH}_3\text{I}_2)(\text{THF})_3$ (**5**) was isolated and structurally characterized in poor yields. Overall, these results offer new examples of how mechanochemistry can be used to rapidly synthesize molecular coordination complexes that are otherwise difficult to prepare using more traditional solution methods.

Introduction

Mechanochemistry,¹⁻¹⁰ defined as a chemical reaction induced by absorption of mechanical energy,¹¹⁻¹² has been used to synthesize coordination complexes and organic chemicals,¹³⁻²⁴ materials,²⁵⁻³² and pharmaceuticals.³³⁻³⁴ The principle advantages of mechanochemistry are that it requires little to no solvent (which can lead to “greener” chemical processes)³⁵⁻³⁶ and it has proven useful for the synthesis of complexes that cannot be prepared using more conventional solution methods.

Although mechanochemistry has seen a resurgence in popularity in recent years,⁸ it has long been used to prepare metal borohydride complexes, including those with f-elements.³⁷⁻³⁸ For example, in 1976 Volkov and Myakishev reported how $U(BH_4)_4$ can be prepared by ball milling UCl_4 with $LiBH_4$.³⁹ More contemporary mechanochemical examples include the synthesis of lanthanide tetrahydroborate salts⁴⁰⁻⁴¹ and highly volatile lanthanide complexes containing chelating borohydrides called aminodiborates.⁴²⁻⁴³ Mechanochemistry has also been used to synthesize organometallic scandium and lanthanide complexes that are difficult to prepare using more conventional methods.⁴⁴⁻⁴⁶

Recently we described how mechanochemistry could be used to improve upon the poor and inconsistent solution yields of a new class of homoleptic phosphinodiboranate complexes with the empirical formula $M(H_3BP^R Bu_2BH_3)_3$ where M = lanthanide or uranium.⁴⁷⁻⁴⁸ In general, phosphinodiboranates are monoanionic borohydride ligands that can be described as two BH_3 groups joined by a phosphido linker (Chart 1), and they are P congeners of the aforementioned aminodiborates.^{42-43,49-54} Phosphinodiboranates have been known for over 50 years with a wide range of different R substituents attached to phosphorus.⁵⁵⁻⁷⁷ However, aside from our previous work with $H_3BP^R Bu_2BH_3^-$ ($^R Bu$ -PDB),⁴⁷⁻⁴⁸ there are few examples of phosphinodiboranate complexes beyond those that have been reported with alkali and alkaline earth metals.^{63,78-79}

Building on our previous effort with $^R Bu$ -PDB, we began to explore the synthesis of lanthanide and actinide complexes with $H_3BPPh_2BH_3^-$ (Ph-PDB) and the unsubstituted phosphinodiboranate $H_3BPH_2BH_3^-$ (H-PDB). These anions have Ph and H substituents that are less electron donating than the alkyl substituents in $^R Bu$ -PDB, and they are presumed to be more weakly coordinating as a result. Only a few structurally characterized metal Ph-PDB complexes have been reported to date: an Fe(II) coordination complex with non-coordinating, outer-sphere Ph-PDB to balance the charge,⁷⁸ a potassium salt with 18-crown-6,⁸⁰ and very recently a heteroleptic magnesium complex prepared *in-situ* by Manners and coworkers.⁷⁹ In contrast, no metal complexes have been structurally characterized with H-PDB. Moreover, H-PDB has been exploited for the development of new ionic liquids, apparently because it is so weakly coordinating.⁸¹

Here we report the mechanochemical synthesis of homoleptic $M(H_3BPPH_2BH_3)_3$ complexes with $M = U$ (**1**), Ce (**2**), Pr (**3**), and Nd (**4**). Using the synthesis of **4** as a representative case study, we compare mechanochemical and solution salt elimination reactions using different solvents and conditions for side-by-side comparison, and we describe the reaction of **4** with THF. Finally, we describe our attempts to prepare H-PDB complexes using similar means along with the structure of the H-PDB coordination complex $U(H_3BPH_2BH_3)_2(THF)_3$ (**5**).

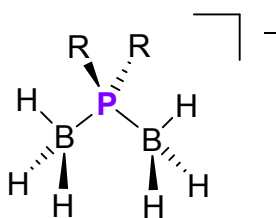
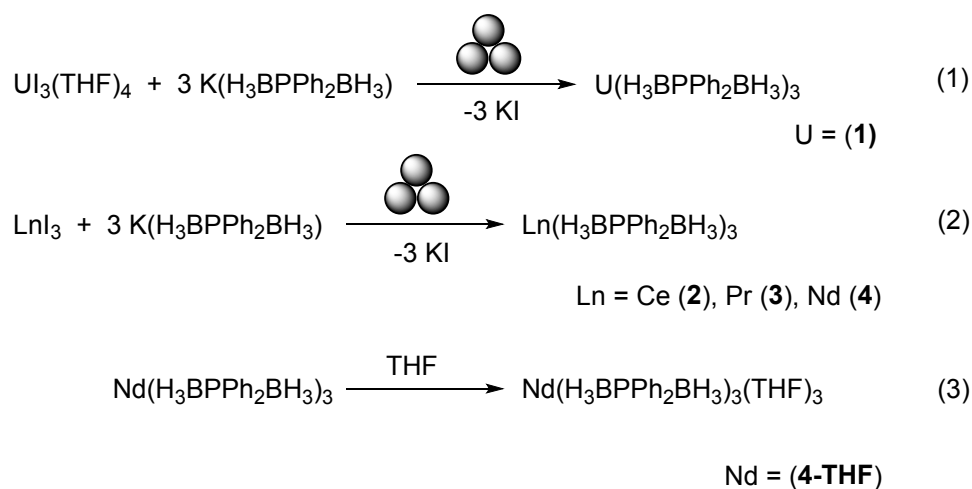


Chart 1. Phosphinodiboranate anions $^R Bu$ -PDB ($R = ^R Bu$), Ph-PDB ($R = Ph$), and H-PDB ($R = H$).

Results and Discussion

Synthesis of Ph-PDB Complexes. The uranium Ph-PDB complex $\text{U}(\text{H}_3\text{BPPPh}_2\text{BH}_3)_3$ (**1**) was prepared by grinding three equiv. of $\text{K}(\text{H}_3\text{BPPPh}_2\text{BH}_3)$ and $\text{U}\text{I}_3(\text{THF})_4$ at 1800 RPM for 90 min using stainless steel balls (Eq 1, Scheme 1). The lanthanide complexes **2** – **4** were prepared similarly using base-free MI_3 where $\text{M} = \text{Ce}^{3+}$, Pr^{3+} , and Nd^{3+} (Eq 2, Scheme 1). Liquid assisted grinding (LAG)⁸² methods were used to prepare all the complexes by adding several drops of Et_2O to the ball mill jars prior to the milling process. The resulting Ph-PDB complexes were separated from the generated KI salt and unreacted starting material by extraction with chlorobenzene or fluorobenzene. All four complexes were crystallized from DCM and Et_2O and isolated in good yields (50 – 80%).



Scheme 1. Mechanochemical synthesis of **1** – **4** and a subsequent conversion of **4** to **4-THF**. The three circles arranged in a triangle are used to indicate ball milling.¹⁶

Attempts to prepare **1** – **4** by mixing the same reagents in THF and Et_2O yielded no visual evidence of reactivity and no isolated product. To better quantify the influence of different solvents on product formation for comparison to our ball milling reactions, we used ^{11}B NMR spectroscopy to investigate reaction mixtures containing three equiv. of $\text{K}(\text{H}_3\text{BPPPh}_2\text{BH}_3)$ and NdI_3 in THF, Et_2O , and chlorobenzene. Data were collected after allowing the mixtures to stir at RT for 24 hrs.

No ^{11}B resonances were observed consistent with $\text{Nd}(\text{H}_3\text{BPPPh}_2\text{BH}_3)_3$ (**4**) or its Lewis base adducts when the reactions were conducted in THF and Et_2O . Only a large peak assigned to the THF-soluble $\text{K}(\text{H}_3\text{BPPPh}_2\text{BH}_3)$ starting material appeared at δ -34.6 ppm in THF (Figure S2; ESI). In contrast, no ^{11}B resonances were detected when the same reactions were conducted in Et_2O , even for $\text{K}(\text{H}_3\text{BPPPh}_2\text{BH}_3)$, which is effectively insoluble in this solvent. For comparison to the differing solubility of $\text{K}(\text{H}_3\text{BPPPh}_2\text{BH}_3)$ in THF and Et_2O , the metal iodide starting materials form etherate adducts that are at least semi-soluble in their corresponding solvents. For example, La Pierre and coworkers reported that the solubility of $\text{NdI}_3(\text{Et}_2\text{O})_3$ in Et_2O is 29.1 mM based on UV-vis measurements.⁸³

We next tried chlorobenzene, which was selected for comparison because Edelstein and coworkers showed that this solvent could be used to prepare base-free $M(\text{MeBH}_3)_4$ where $M = \text{Zr}$, Th , U , and Np by treating the corresponding $M\text{Cl}_4$ with 4 equiv. of $\text{Li}(\text{MeBH}_3)$.⁸⁴ In contrast to the reactions conducted in THF and Et_2O , stirring three equiv. of $\text{K}(\text{H}_3\text{BPPPh}_2\text{BH}_3)$ and NdI_3 in chlorobenzene for 24 h at RT yielded a small ^{11}B NMR resonance at δ 95.3 ppm consistent with the formation of **4** (Figure 1). Increasing the starting temperature to 50 °C yielded slightly more **4**, but also revealed evidence of decomposition. Performing the reaction at 100 °C yielded no evidence of **4**; only resonances attributed to decomposition were observed.

To compare the solution results side-by-side with our mechanochemical results, we ball milled NdI_3 with three equiv. of $\text{K}(\text{H}_3\text{BPPPh}_2\text{BH}_3)_3$ at 1800 RPM for 90 min at the same scale as our reactions using organic solvents. The residue was extracted with the same volume of chlorobenzene used in our solvent study (Figure 1). Analysis of the extract by ^{11}B NMR spectroscopy showed a higher concentration of the resonance at δ 95.3 ppm as well as the two new features at δ 75.6 and 176.5 ppm. These are the same ^{11}B resonances observed when analytically pure crystals of **4** are dissolved in chlorobenzene (the assignment of these three resonances will be described below). These results demonstrate how the mechanochemical reactions are higher yielding and faster than comparable reactions performed in solution.

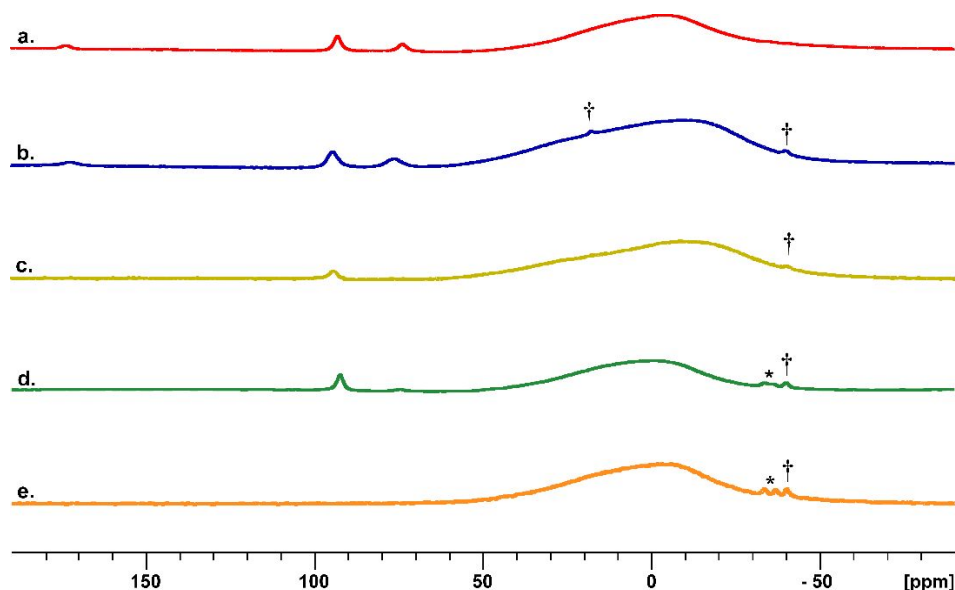


Figure 1. ^{11}B NMR spectra of a) crystalline $\text{Nd}(\text{H}_3\text{BPPPh}_2\text{BH}_3)_3$ (**4**) dissolved in chlorobenzene; b) chlorobenzene extract (20 mL) from ball-milled reaction mixture of NdI_3 with three equiv. of $\text{K}(\text{H}_3\text{BPPPh}_2\text{BH}_3)$; c) mixture of NdI_3 and three equiv. of $\text{K}(\text{H}_3\text{BPPPh}_2\text{BH}_3)$ stirred in 20 mL of chlorobenzene for 24 h at RT; d) same mixture as c stirred for 24 h at 50 °C; e) same mixture as c stirred for 24 h at 100 °C. The * is assigned to decomposition products generated at elevated temperatures. The † is assigned to small amounts of hydrolysis or starting material. The large broad feature centered around δ 0 ppm is attributed to borosilicate inside the instrument.

XRD studies of homoleptic Ph-PDB complexes. Single-crystal X-ray diffraction (XRD) studies were carried out to investigate the structures **1** – **4**. Two types of crystals with slightly

different morphologies were observed for **1**, and XRD studies revealed these to be different structural isomers (Figure 2). The first structure, which is designated as **1a** (Chart 2), is a coordination polymer with each uranium coordinated to one chelating Ph-PDB and four bridging Ph-PDB ligands that link together adjacent uranium ions in the unit cell. The geometry around U is distorted octahedral based on the arrangement of the six boron atoms with the largest B-U-B angles being $147.0(2)^\circ$, $165.5(2)^\circ$, and $173.8(2)^\circ$. The second structural isomer of $U(H_3BPPH_2BH_3)_3$ (**1b**) is a dimer similar to the structure reported previously for the 'Bu-PDB complex $U(H_3BP'Bu_2BH_3)_3$. The geometry around U in **1b** is distorted trigonal prismatic again based on the arrangement of boron atoms and as indicated by the more acute B-U-B angles of $137.4(6)^\circ$, $143.9(2)^\circ$, and $154.3(7)^\circ$ compared to those in **1a**.

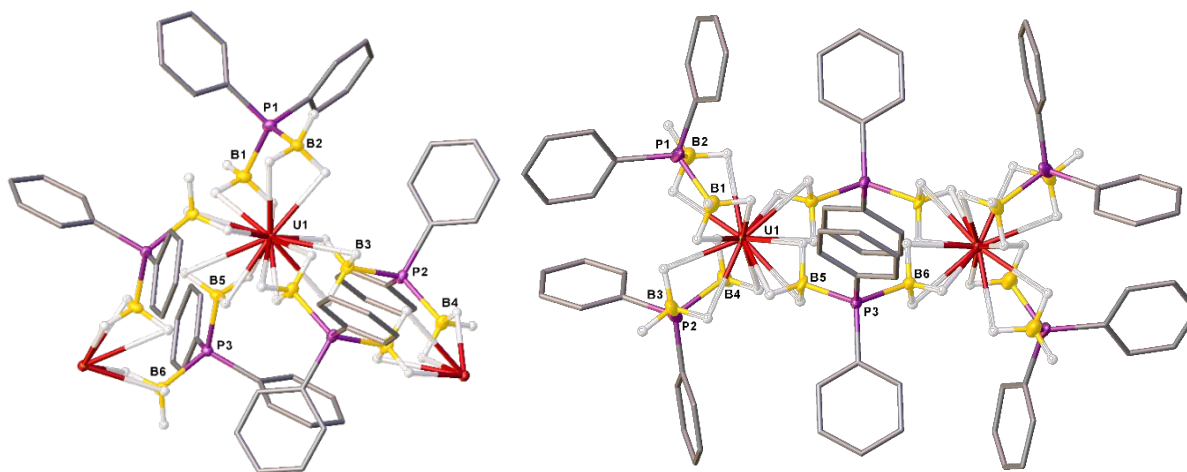


Figure 2. Structural isomers **1a** (left) and **1b** (right) of $U(H_3BPPH_2BH_3)_3$. Ellipsoids shown at 35% probability. The phenyl rings are represented as pipes and hydrogens attached to carbon are omitted for clarity.

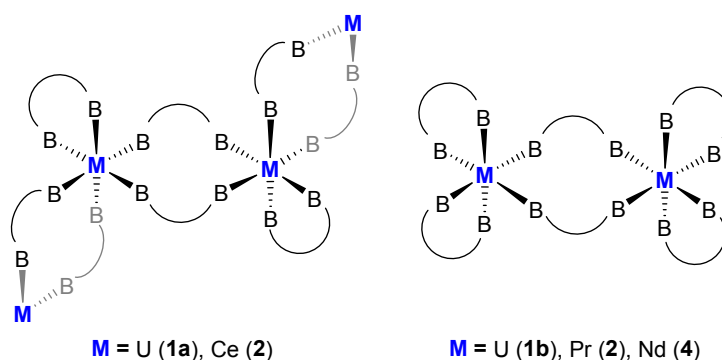


Chart 2. Simplified structural framework of **1** – **4**. B – B = $H_3BPPH_2BH_3^-$.

The structure of $Ce(H_3BPPH_2BH_3)_3$ (**2**) with the largest lanthanide in our series is identical to polymeric **1a** (Figure 3) with one chelating Ph-PDB and four Ph-PDB ligands bridging to adjacent cerium ions, whereas the structures of $Pr(H_3BPPH_2BH_3)_3$ (**3**) and $Nd(H_3BPPH_2BH_3)_3$ (**4**) are both dimers like **1b**. Both **3** and **4** crystallize in the monoclinic space group $P2_1/c$ but subtle differences are observed in the two structures presumably due to the differences in ionic radii for Pr^{3+} (0.99 Å) and Nd^{3+} (0.983 Å).⁸⁵ The structure of **4** contains a mirror plane so that half of the dimer

represents the smallest asymmetric unit (one metal, one bridging Ph-PDB, and two chelating Ph-PDB ligands) (Figure 4). The mirror plane is lost as the metal ion size increases in **3** so that all atoms in the dimer are symmetrically inequivalent.

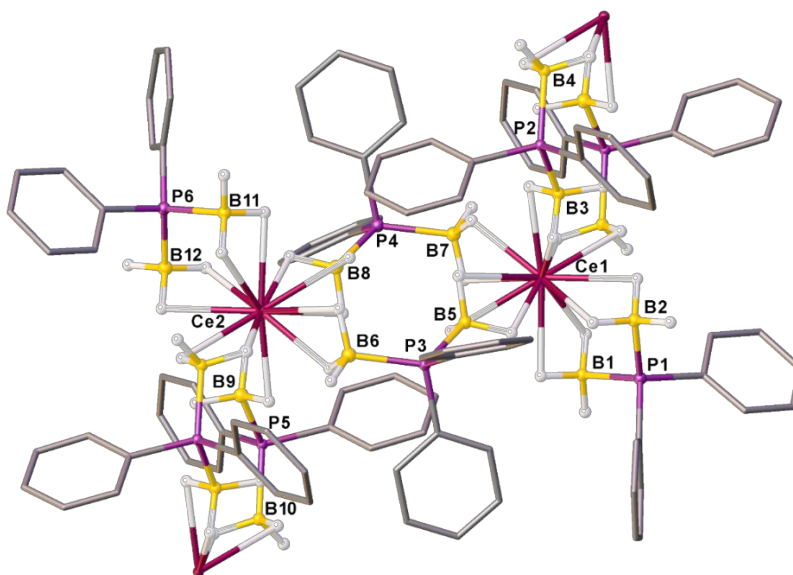


Figure 3. Molecular structure of $\text{Ce}(\text{H}_3\text{BPPPh}_2\text{BH}_3)_3$ (**2**). Ellipsoids shown at 35% probability. The phenyl rings are represented as pipes and all hydrogens attached to carbon are omitted for clarity.

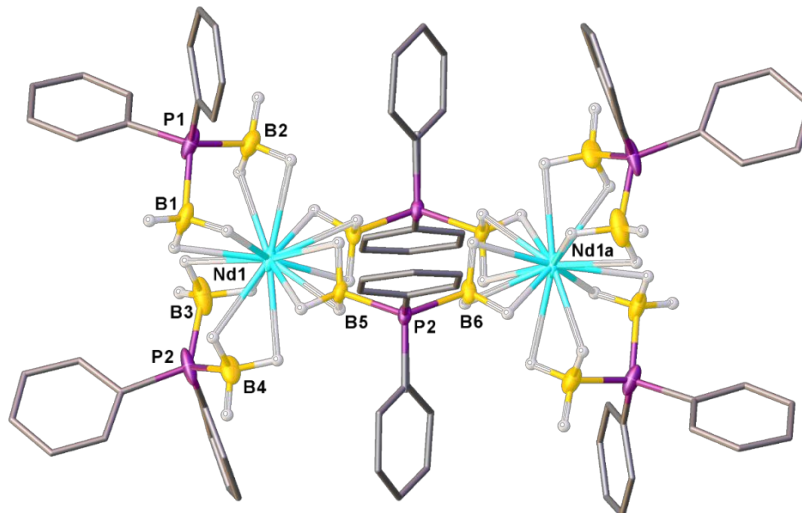


Figure 4. Molecular structure of $\text{Nd}(\text{H}_3\text{BPPPh}_2\text{BH}_3)_3$ (**4**). Ellipsoids shown at 35% probability. The phenyl rings are represented as pipes and hydrogens attached to carbon are omitted for clarity.

Given the difficulties accurately assigning the position of hydrogen atoms using single-crystal XRD, metal-boron bond distances are often used to estimate the denticity of borohydride ligands and determine the overall metal coordination number.⁸⁶ To facilitate this analysis and show how the M-B bond distances change as a function of metal radii and structure type (polymer vs. dimer), we plotted the M-B distances as a function of the ionic radii (Figure 5). Plotting the M-B distance

data this way reveals clustering indicative of the different BH_3 coordination modes (κ^1 , κ^2 , or κ^3) and denticities for Ph-PDB (Chart 3). Starting with the structural isomers of $\text{U}(\text{H}_3\text{BPPH}_2\text{BH}_3)_3$ **1a** and **1b**, at least two M-B groupings are observed. The U-B distances between 2.683(8) – 2.747(7) Å are consistent with κ^3 - BH_3 coordination based on comparison to U-B distances and corresponding BH_3 denticities reported with U^{3+} .^{52,87-88} The second grouping spans a slightly larger range from 2.892(6) – 3.04(4) Å. These values are consistent primarily with κ^2 denticity,^{52,87} although the largest M-B bond distance at 3.04(4) Å may be κ^1 because it is slightly beyond what is typically reported for κ^2 - BH_3 with U^{3+} . The structures of **2** – **4** show similar distributions of M-B distances, but the scatter of the longest bond distances become smaller as the radii decreases. Overall, the summation of the M-B distances suggest that the coordination numbers are 13 – 14, which is consistent with those observed previously for trivalent lanthanide and actinide 'Bu-PDB,⁴⁷⁻⁴⁸ as well as other borohydride complexes.^{43,52,87,89-91}

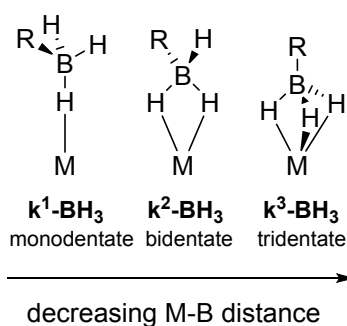


Chart 3. Comparison of B-H denticity and M-B distance.

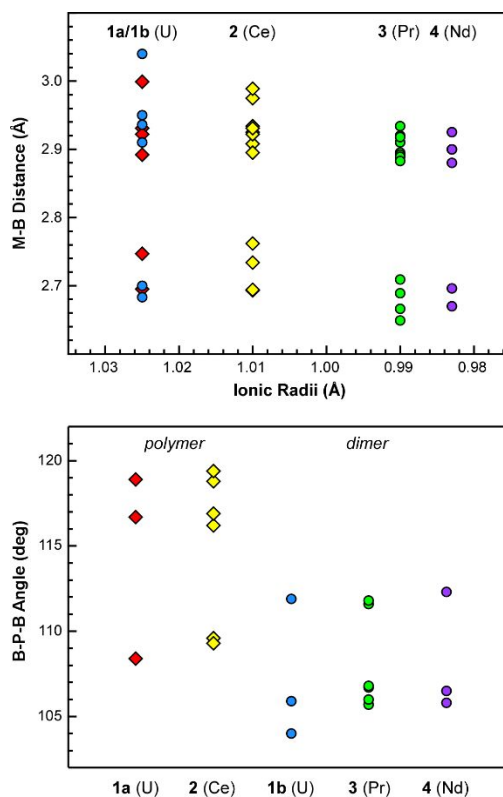


Figure 5. Metal-boron (M-B) distances (*top*) and B-P-B angles (*bottom*) from single-crystal XRD data. Data points for polymeric structures are represented as diamonds whereas those for dimeric structures are represented as spheres.

One of the more significant differences between the Ph-PDB structures is the B-P-B angles, which show remarkable flexibility and vary by as much as 15.4° . The polymeric structures for **1a** and **2** have larger chelating and bridging B-P-B angles compared to the dimeric structures for **1b**, **3**, and **4** (Figure 5). The chelating B-P-B angles in the dimeric structures average $105.9(4)^\circ$, whereas those in the polymeric structures average $109.1(2)^\circ$. Likewise, the bridging B-P-B angles in the dimers average $111.9(2)^\circ$, which is significantly smaller than the average bridging B-P-B angles in the polymeric structures at $117.8(2)^\circ$. In general, Ph-PDB can access a wider range of B-P-B angles than previously observed with *t*-Bu-PDB complexes, which only vary by as much as 7.8° . Furthermore, all homoleptic *t*-Bu-PDB complexes structurally characterized to date with trivalent f-metals – even those with U^{3+} and Ce^{3+} – exist as dimers in the solid state. We attribute these structural differences with Ph-PDB and *t*-Bu-PDB to the decreased steric profile afforded by phenyl substituents vs. *tert*-butyl, which can rotate and adopt different conformations to afford a wider range of B-P-B angles.

Synthesis and structure of $Nd(H_3BPPPh_2BH_3)_3(THF)_3$. We have shown in previous studies that the *t*-Bu-PDB complexes $U(H_3BP^tBu_2BH_3)_3$ and $Nd(H_3BP^tBu_2BH_3)_3$ could be crystallized as base-free dimers from THF-containing solutions.⁴⁷ In contrast, *t*-Bu-PDB complexes with smaller lanthanides such as $Tb(H_3BP^tBu_2BH_3)_3$, $Er(H_3BP^tBu_2BH_3)_3$, and $Lu(H_3BP^tBu_2BH_3)_3$ all formed monomeric complexes with the formula $M(H_3BP^tBu_2BH_3)_3(THF)_3$, where $M = Tb, Er, \text{ and } Lu$.⁴⁷ Dissolving crystals of $Nd(H_3BPPPh_2BH_3)_3$ (**4**) in THF clearly yielded different ^{11}B resonances compared to those for **4**, which suggested that a new complex was formed. Indeed, this was confirmed by addition of Et_2O to the THF solutions, which yielded light purple XRD quality crystals of $Nd(H_3BPPPh_2BH_3)_3(THF)_3$ (**4-THF**; Figure 6).

The coordination geometry of **4-THF** is pentagonal bipyramidal based on the arrangement of the boron and oxygen atoms around Nd. This differs from the THF adducts previously observed with *t*-Bu-PDB complexes containing smaller lanthanides because it contains two dangling and one chelating Ph-PDB ligands (Figure 6). These structural differences are likely attributed to the increased radii and larger coordination sphere of Nd^{3+} compared to Tb^{3+} , Er^{3+} , and Lu^{3+} . The chelating Ph-PDB ligand in **4-THF** lies in the equatorial plane with the three THF molecules. Both BH_3 groups are bound in a κ^2 coordination with representative Nd-B distances of 2.990(9) and 2.908(8) Å. The two dangling Ph-PDB ligands occupy the axial positions with each BH_3 group bound in a tridentate fashion, as indicated by the shorter Nd-B distances of 2.678(8) and 2.791(7) Å (Table 1). The average Nd-O bond distance of 2.49(3) Å is consistent with other Nd^{3+} complexes containing THF ligands. The overall coordination number of **4-THF** is 13 when considering the denticity of the BH_3 groups.

Despite the different substituents attached to phosphorus, the B-P-B angles and associated intramolecular $B\cdots B$ distances in the dangling Ph-PDB ligands in **4-THF** and *t*-Bu-PDB complexes such as $Er(H_3BP^tBu_2BH_3)_3(THF)_3$ are effectively identical in the absence of chelation or intermolecular bridging modes.

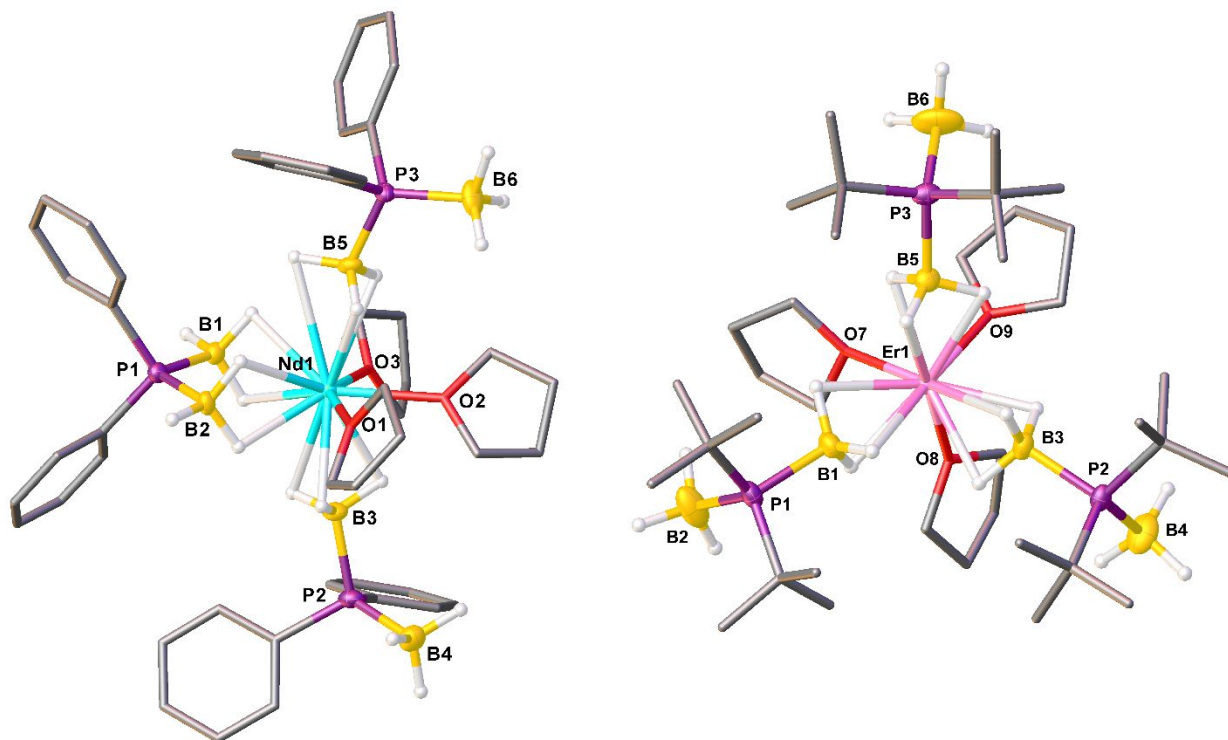


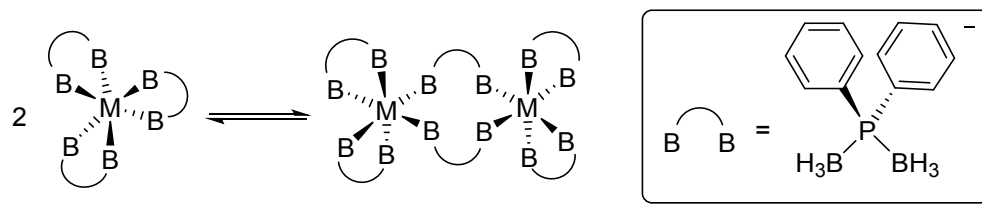
Figure 6. Single-crystal XRD structure comparison between $\text{Nd}(\text{H}_3\text{BPPPh}_2\text{BH}_3)_3(\text{THF})_3$ (**4-THF**; *left*) and $\text{Er}(\text{H}_3\text{BP}^t\text{Bu}_2\text{BH}_3)_3(\text{THF})_3$ (*right*).⁴⁷ Thermal ellipsoids are drawn with 35% probability. All phenyl rings, *tert*-butyl groups, and THF molecules are represented as pipes and all hydrogen atoms attached to carbon were omitted from the figure.

Table 1. Bond distance and angle measurements for $\text{Nd}(\text{H}_3\text{BPPPh}_2\text{BH}_3)_3(\text{THF})_3$ (**4-THF**).

Ln-B	Ln-O	B···B	B-P-B	B-Nd-B	B-Ln-O	B-Ln-O	B-Ln-O	B-Ln-O
2.990(9)	2.47(1)	3.112(9)	107.5(3)	63.7(2)	94.7(2)	151.9(2)	74.8(2)	87.1(3)
2.908(8)	2.479(5)	3.24(1)	114.6(4)	98.8(2)	96.7(2)	137.4(3)	73.9(3)	91.0(3)
2.678(8)	2.506(3)	3.22(1)	115.1(4)	91.0(2)	167.4(2)	144.0(2)	84.6(2)	82.3(2)
2.791(7)						137.9(2)	85.3(2)	90.4(2)

Spectroscopic Analysis of Ph-PDB Complexes. ^1H and ^{11}B NMR data were collected on all the Ph-PDB complexes to analyze their structures in solution. As reported for ^tBu -PDB complexes, and despite the differences in solid-state structures, homoleptic Ph-PDB complexes appear to exist as a mixture of monomers and dimers in solution (Scheme 2).⁴⁷⁻⁴⁸ The ^1H and ^{11}B NMR spectra revealed three paramagnetically shifted resonances for each compound (Table 2). Two of these resonances exist in a 1:2 ratio consistent with the different chemical environments expected for the bridging and chelating Ph-PDB ligands in the dimer, whereas the remaining resonance is assigned to chemically equivalent Ph-PDB ligands in the monomer. The ^1H NMR spectra also showed a range of different phenyl resonances, although these were less paramagnetically shifted

than the BH_3 resonances and more difficult to assign due to the mixture of monomer and dimer, different hydrogen positions on each phenyl group, and associated overlap of different resonances.



Scheme 2. Comparison of monomeric and dimeric phosphinodiboranate complexes presumed to exist in solution.

Table 2. Room Temperature ^1H and ^{11}B NMR data of BH_3 resonances (δ , ppm) for Ph-PDB complexes in CD_2Cl_2 .

complex	Dimer		Monomer	
	^1H	^{11}B	^1H	^{11}B
1	70.2, 94.1	130.7, 308.4	93.0	186.3
2	20.8, 33.1	3.1, 44.0	23.8	11.4
3	55.8, 79.0	46.3, 147.2	63.8	66.1
4	77.3, 83.5	75.6, 176.5	78.3	95.3
4-THF	64.8, 50.6	55.0, 71.8	47.6	45.4

^{11}B NMR data for the THF bound and unbound species, **4-THF** and **4**, respectively show very different NMR spectra in CD_2Cl_2 (Figure 7). As noted above, $\text{Nd}(\text{H}_3\text{BPPPh}_2\text{BH}_3)_3$ shows three well defined resonances with the BH_3 resonances of the chelating and bridging Ph-PDB ligands of the dimer at δ 176.5 and 75.6, respectively. The middle resonance at δ 95.3 is assigned to the monomer. In contrast, the ^{11}B NMR spectrum of **4-THF** shows upfield shifts. Three features are again observed, which is consistent with the presence of three unique ^{11}B environments in the monomeric structure of **4-THF**.

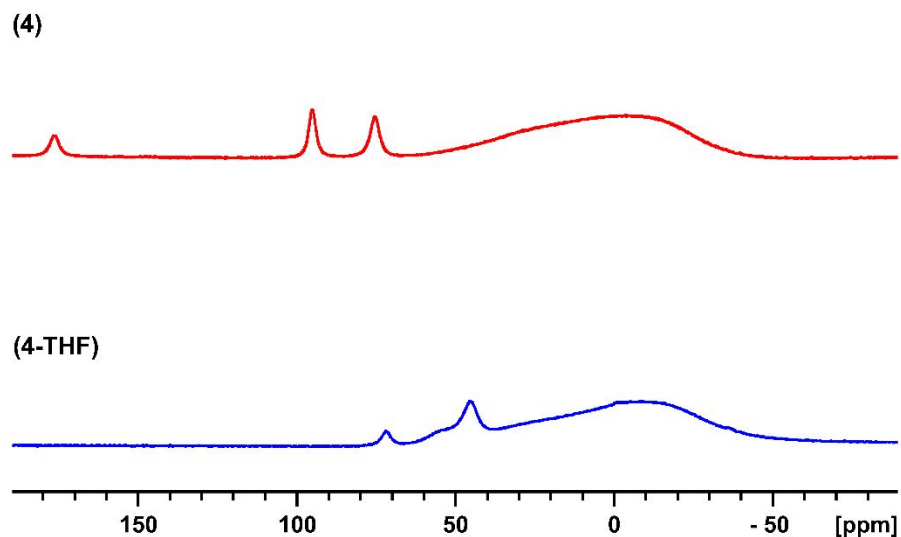


Figure 7. ^{11}B NMR stack plot of $\text{Nd}(\text{H}_3\text{BPPPh}_2\text{BH}_3)_3$ (**4**) and $\text{Nd}(\text{H}_3\text{BPPPh}_2\text{BH}_3)_3(\text{THF})_3$ (**4-THF**). Data for both complexes were collected in CD_2Cl_2 . The large broad feature centered around δ 0 ppm is attributed to borosilicate inside the instrument.

Solid-state IR data were collected for Ph-PDB complexes to assess the effect that structure and THF binding have on molecular vibrations, especially B-H stretching frequencies that appear between 2200 cm^{-1} and 2500 cm^{-1} (Figure 8). Spectra collected on the homoleptic base-free complexes show only subtle variations across the series despite the structural differences between the polymers (**1a** and **2**) and the dimers (**1b**, **3**, and **4**). Each spectrum yielded a strong B-H stretching band centered around 2250 cm^{-1} that is assigned to bridging B-H-M stretches. Two more resolved, albeit less intense vibrations, were observed at higher wavenumbers and assigned to terminal B-H stretches (ca. 2440 cm^{-1}). In contrast to the base-free complexes, the IR spectrum of **4-THF** revealed new B-H stretches at 2331 and 2358 cm^{-1} consistent with the dangling BH_3 groups. The spectrum of **4-THF** also revealed the diagnostic symmetric and asymmetric C-O-C vibrations associated with THF at 853 and 1003 cm^{-1} , respectively, and additional C-H stretches centered around 3000 cm^{-1} .

As previously observed for the $\text{M}(\text{H}_3\text{BP}^i\text{Bu}_2\text{BH}_3)_3(\text{THF})_3$ complexes with ^iBu -PDB, the THF molecules in **4-THF** can be displaced to some extent by placing the samples under vacuum or by vigorously grinding the sample with KBr. This was observed during our initial attempts to prepare IR samples of **4-THF** as KBr pellets. These samples yielded spectra identical to the base free complex **4** and showed no THF vibrations. For this reason, the solid-state IR spectrum of **4-THF** was only lightly ground prior to pellet formation.

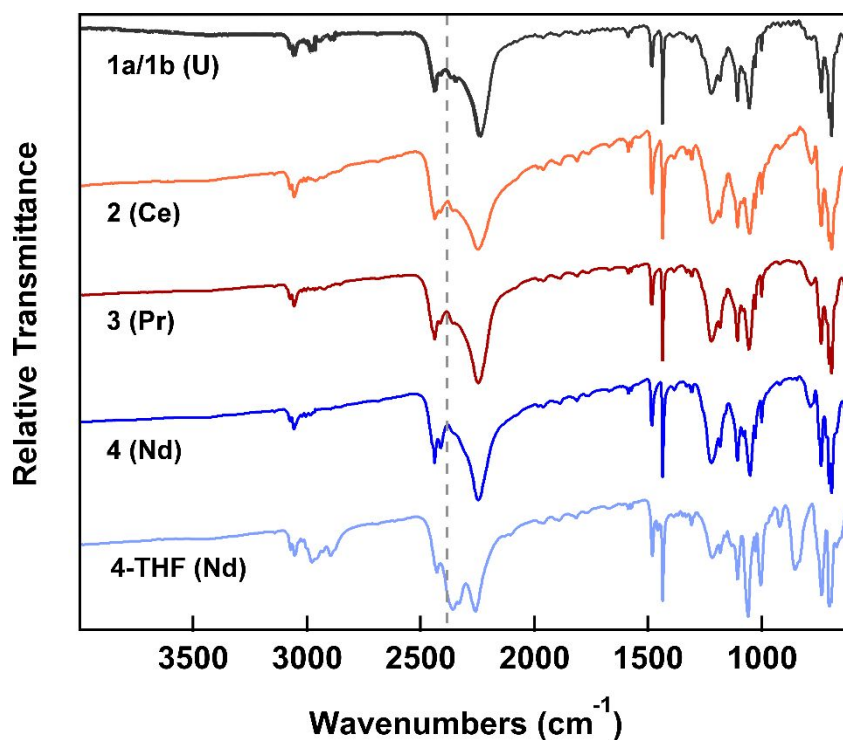
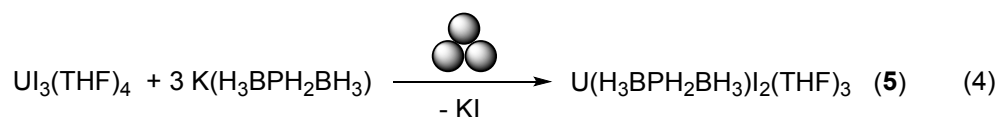


Figure 8. Comparison of solid-state IR data (KBr) for **1a/1b**, **2**, **3**, **4**, and **4-THF**. The gray dashed line was added at 2400 cm^{-1} for reference.

Synthesis and XRD Studies of $\text{U}(\text{H}_3\text{BPH}_2\text{BH}_3)_2(\text{THF})_3$. In sharp contrast to our results with $\text{K}(\text{H}_3\text{BPPH}_2\text{BH}_3)$, attempts to prepare homoleptic H-PDB complexes using $\text{K}(\text{H}_3\text{BPH}_2\text{BH}_3)$ yielded only limited results. For example, grinding $\text{UI}_3(\text{THF})_4$ with three equivalence of $\text{K}(\text{H}_3\text{BPH}_2\text{BH}_3)$ yielded only the partial metathesis product $\text{U}(\text{H}_3\text{BPH}_2\text{BH}_3)_2(\text{THF})_3$ (**5**) as shown in Scheme 3. The complex was isolated by extraction from chlorobenzene and subsequently crystallized from THF and pentane in very low yields ($\leq 5\%$). Attempts to use other extracting solvents (Et_2O , DCM, and fluorobenzene) yielded no soluble product. Synthesis of the neodymium congener by the same method was also attempted, but the reaction was poor yielding and not enough material could be extracted to obtain single crystals.



Scheme 3. Mechanochemical synthesis of **5**. The three circles arranged in a triangle are used to indicate ball milling.¹⁶

Single-crystal XRD studies of **5** revealed a distorted pentagonal bipyramidal coordination geometry with the two iodide ligands in the axial positions and the H-PDB and THF ligands occupying the equatorial plane (Figure 9). The U-B distances of 2.965 Å indicate κ^2 coordination of the BH_3 groups, as observed in **1a** and **1b**. The B-U-B and average O-U-O angles are 63.1° and 78.4(4)°, respectively. The *trans* I-U-I bond angle is slightly bent at 164.3(4)°. The H-PDB anion has a B-P-B angle of 106.7(8)°, which is close to the angle observed for the chelating B-P-B angles

in both $\text{U}(\text{H}_3\text{BPPH}_2\text{BH}_3)_3$ structures (**1a** and **1b**). Remarkably, this structure is similar to $\text{Er}(\text{H}_3\text{BNH}_2\text{BH}_3)\text{Cl}_2(\text{THF})_3$ containing the unsubstituted aminodiboranate (and N congener) $\text{H}_3\text{BNH}_2\text{BH}_3^-$.⁵³ It worth noting that $\text{Er}(\text{H}_3\text{BNH}_2\text{BH}_3)\text{Cl}_2(\text{THF})_3$ was also isolated as an incomplete metathesis product in attempts to prepare $\text{Er}(\text{H}_3\text{BNH}_2\text{BH}_3)_3$, and similar results have been observed with $\text{Nd}(\text{H}_3\text{BNMe}_2\text{BH}_3)\text{Cl}_2(\text{THF})_3$ (see below).⁵⁴

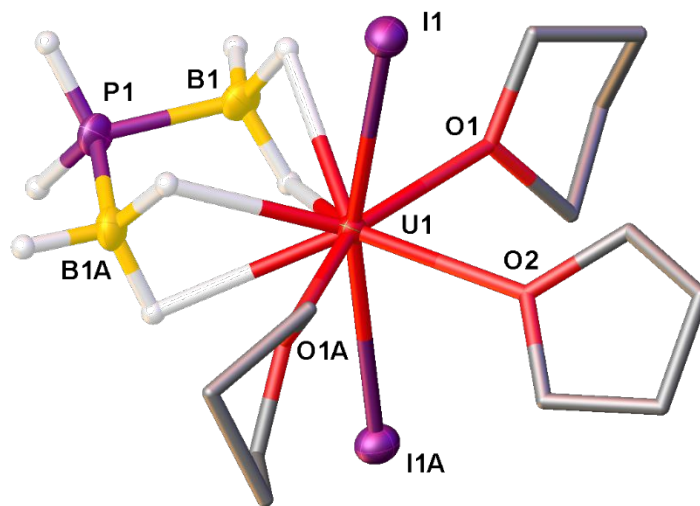


Figure 9. Single crystal XRD structure of $\text{U}(\text{H}_3\text{BPH}_2\text{BH}_3)\text{I}_2(\text{THF})_3$ (**5**). Thermal ellipsoids represented at 35% probability. All THF molecules are represented as pipe bonds and all hydrogens off the THF molecules have been omitted for clarity. A symmetry plane lies across complex **5**.

Conclusion

In summary, we have demonstrated how mechanochemistry can be used to overcome limited solution reactivity for the synthesis of *f*-metal phosphinodiboranate complexes $\text{U}(\text{H}_3\text{BPPH}_2\text{BH}_3)_3$ (**1**), $\text{Ce}(\text{H}_3\text{BPPH}_2\text{BH}_3)_3$ (**2**), $\text{Pr}(\text{H}_3\text{BPPH}_2\text{BH}_3)_3$ (**3**), and $\text{Nd}(\text{H}_3\text{BPPH}_2\text{BH}_3)_3$ (**4**). Single-crystal XRD studies showed that these complexes exist as coordination polymers (**1a** and **2**) or dimers (**1b**, **3**, and **4**) in the solid state, but they depolymerize and appear to exist as mixtures of monomers and dimers in solution according to ^1H and ^{11}B NMR studies. Despite the success with Ph-PDB, only the partial metathesis product $\text{U}(\text{H}_3\text{BPPH}_2\text{BH}_3)\text{I}_2(\text{THF})_2$ (**5**) was isolated and structurally characterized when similar mechanochemical reactions were attempted using the unsubstituted phosphinodiboranate H-PDB. This observation suggests that H-PDB may be more weakly coordinating than Ph-PDB, consistent with its prior use as a non-coordinating anion in ionic liquids.⁸¹

The biggest question that remains from these studies is: why do metathesis reactions with PDB salts work when performed under mechanochemical conditions but fail when performed in solution, especially with THF or Et_2O ? We can speculate on this question by comparing our results

to studies with aminodiboranates (*i.e.* the nitrogen congeners of phosphinodiboranates) that showed how salt elimination reactions with trivalent *f*-metal halides can be attenuated (and even reversed!) when performed in coordinating solvents. It was recently reported that mixing NdCl_3 with three equiv. of $\text{Na}(\text{H}_3\text{BNMe}_2\text{BH}_3)$ in THF yields a mixture containing the partial metathesis product $\text{Nd}(\text{H}_3\text{BNMe}_2\text{BH}_3)\text{Cl}_2(\text{THF})_3$.⁵⁴ Subsequent removal of the solvent from the mixture – which still contained unreacted $\text{Na}(\text{H}_3\text{BNMe}_2\text{BH}_3)$ – followed by addition of non-coordinating pentane to the solid residue allowed the metathesis reactions to proceed to completion with rapid formation of $\text{Nd}(\text{H}_3\text{BNMe}_2\text{BH}_3)_3(\text{THF})$.⁵⁴ More remarkably, it was shown that dissolving the trisubstituted complex $\text{Nd}(\text{H}_3\text{BNMe}_2\text{BH}_3)_3(\text{THF})$ in THF with excess NaCl – which has very low solubility in THF (6 mg/L)⁵⁴ – yielded $\text{Nd}(\text{H}_3\text{BNMe}_2\text{BH}_3)\text{Cl}_2(\text{THF})_3$ with elimination of 2 equiv. of $\text{Na}(\text{H}_3\text{BNMe}_2\text{BH}_3)$. These results clearly indicate that $\text{Nd}(\text{H}_3\text{BNMe}_2\text{BH}_3)\text{Cl}_2(\text{THF})_3$ is the thermodynamically-favored product in THF when both NaCl and $\text{Na}(\text{H}_3\text{BNMe}_2\text{BH}_3)$ are present. Interestingly, performing the same reaction by mixing NdCl_3 with three equiv. of $\text{Na}(\text{H}_3\text{BNMe}_2\text{BH}_3)$ in more weakly-coordinating Et_2O instead of THF allowed the metathesis reaction to proceed to completion to form $\text{Nd}(\text{H}_3\text{BNMe}_2\text{BH}_3)_3$. Similar solvent-dependent differences in salt elimination reactivity were observed for the synthesis of $\text{U}(\text{H}_3\text{BNMe}_2\text{BH}_3)_3(\text{THF})$ and $\text{U}(\text{H}_3\text{BNMe}_2\text{BH}_3)_3$ in THF and Et_2O , respectively.⁵²

While different thermodynamic (*e.g.*, solvation, lattice energy, metal-ligand bond strength) and kinetic factors contribute to determining whether a metathesis reaction occurs,⁵⁴ a key factor governing these reactions appears to be the strength of metal-solvent coordination relative to the incoming ligand. Donor solvents, which also exist in large excess in solution-phase reactions, must be displaced from the metal along with the corresponding halide for a metathesis reaction to proceed. Compared to reactions with $\text{Na}(\text{H}_3\text{BNMe}_2\text{BH}_3)$, this appears to be even more problematic for the potassium Ph-PDB and H-PDB salts, which did not exhibit any observable reactivity in THF or Et_2O with the trivalent *f*-metal iodides tested here. The metathesis reactions do proceed slowly in chlorobenzene, but also fail to go completion at RT within 24 h, which suggests that even chlorobenzene may impede reaction progress in solution. In the context of our hypothesis, it has been shown that neutral, substituted benzenes like chlorobenzene can coordinate to trivalent *f*-metals,⁹²⁻⁹³ and examples of arene-bound U^{3+} complexes containing borohydride ligands have been structurally characterized.⁹⁴⁻⁹⁵ More work is needed to test this hypothesis and fully elaborate all the factors contributing to limited PDB salt metathesis reactivity in solution. Nevertheless, the comparative solution and solid-state Ph-PDB studies described here clearly demonstrate how mechanochemistry can provide convenient access to metal complexes that are otherwise difficult to prepare by conventional solution methods.

Experimental

General considerations. All reactions were carried out under an atmosphere of N_2 using glovebox or standard Schlenk techniques. All glassware was heated at 150 °C for at least two hours and allowed to cool under vacuum before use. Solvents were dried and deoxygenated using a Pure Process Technologies Solvent Purification System and stored over 3 Å molecular sieves. Deuterated solvents were deoxygenated on the Schlenk line by three freeze–pump–thaw cycles and stored over 3 Å molecular sieves for at least 3 days before use. $\text{K}(\text{H}_3\text{BPPPh}_2\text{BH}_3)$ was prepared from commercially available starting materials using the method described by Wagner and

coworkers.⁷³ $\text{UI}_3(\text{THF})_4$ was prepared from $\text{UI}_3(1,4\text{-dioxane})_{1.5}$, as described by Kiplinger and coworkers,⁹⁶ or from UCl_4 as described previously.⁹⁷ Anhydrous LnI_3 salts were purchased from Alfa Aesar or Strem Chemicals and used as received.

^1H NMR data were collected on a Bruker AVANCE-400 operating at 400 MHz, or a Bruker AVANCE-500 operating at 500 MHz. The ^{11}B NMR data were collected on a Bruker AVANCE-400 operating at 128 MHz or a Bruker AVANCE-500 operating at 160 MHz. Chemical shifts are reported in δ units relative to residual NMR solvent peaks (^1H) and $\text{BF}_3 \cdot \text{Et}_2\text{O}$ (^{11}B ; δ 0.0 ppm). ^{31}P NMR resonances were not observed for any of the metal complexes presumably because of unresolved peak broadening in the presence of paramagnetic metals and quadrupolar coupling with the boron nuclei (^{11}B and ^{10}B). Microanalytical data (CHN) were collected using an EAI CE-440 elemental analyzer at the University of Iowa's Shared Instrumentation Facility. CHN analysis for all the complexes gave satisfactory %H, but %C data were consistently 2 - 4% lower than expected for all the complexes, which may be attributed to metal-carbide formation during combustion. IR spectra were acquired with a Thermo Scientific Nicolet iS5 in an N_2 -filled glovebox as KBr pellets and using an ATR accessory. Mechanochemical synthesis was carried out on a Form-Tech Scientific (FTS) FTS1000 shaker mill operating at 1800 rpm. All mechanochemical reactions were conducted in 5 mL stainless steel "SmartSnap" (hermetic seal) grinding jars using two 5 mm stainless steel balls (304 grade) for grinding. The average weight of the balls was 0.522 ± 0.002 g based on measurement and averaging of 5 samples.

Tris(diphenylphosphinodiboranato)uranium(III), $\text{U}(\text{H}_3\text{BPPPh}_2\text{BH}_3)_3$ (1). $\text{UI}_3(\text{THF})_4$ (0.101 g, 0.111 mmol) and $\text{K}(\text{H}_3\text{BPPPh}_2\text{BH}_3)$ (0.0834 g, 0.331 mmol) were loaded into a 5 mL FTS ball milling jar with two 5 mm stainless steel balls and several drops of Et_2O . The jar was hermetically sealed, transferred to an FTS shaker mill, and milled for 90 minutes. The jar was then transferred to a glovebox and opened to reveal a dark red residue. The contents were scraped into an 11-dram vial equipped with a stir bar and stirred in 40 mL of fluorobenzene for 30 minutes. The suspension was filtered through a fine frit and evaporated to dryness under vacuum to reveal a red oily solid. The solid was dissolved in the minimal amount of DCM (ca. 1 mL) and slowly diffused with Et_2O to afford small dark red needles (38 mg). Yield: 46%. Anal. Calcd. For $\text{C}_{36}\text{H}_{48}\text{B}_6\text{P}_3\text{U}$: H, 5.52. Found: H, 5.46%. ^1H NMR (500 MHz, CD_2Cl_2): δ 6.79, 7.30, 7.47, 7.59, 7.73, 8.09, 8.24, (br s, Ph), 70.2 (br s, FWHM = 640 Hz, BH_3 , dimer), 93.0 (br s, FWHM = 550, 18 H, BH_3 , monomer), 94.1 (br s, FWHM = 470, 12H, BH_3 , dimer). ^{11}B NMR (160 MHz, CD_2Cl_2): δ 130.7 (br s, FWHM = 500 Hz, BH_3 , dimer), 186.3 (br s, FWHM = 660, BH_3 , monomer), 308.4 (br s, FWHM = 380 Hz, BH_3 , dimer). IR (KBr) $\bar{\nu}_{\text{max}}$ (cm^{-1}): 3075 (w), 3058 (w), 3006 (w), 2928 (w), 2853 (w), 2435 (m), 2412 (m), 2236 (s), 1981 (w), 1962 (w), 1885 (w), 1812 (w), 1761 (w), 1672 (w), 1586 (w), 1573 (w), 1482 (m), 1435 (s), 1384 (w), 1330 (w), 1307 (w), 1214 (s), 1183 (s), 1106(s), 1047 (s), 1027 (m), 999 (m), 921 (w), 845 (w), 780 (w), 746 (s), 746 (s), 701 (s), 690 (s), 622 (m), 612 (m).

Tris(diphenylphosphinodiboranato)cerium(III), $\text{Ce}(\text{H}_3\text{BPPPh}_2\text{BH}_3)_3$ (2). Prepared as described for **1** with CeI_3 (0.103 g, 0.198 mmol) and $\text{K}(\text{H}_3\text{BP}^i\text{Bu}_2\text{BH}_3)$ (0.145 g, 0.575 mmol). Yield: 53 mg (52%). Anal. Calcd. For $\text{C}_{36}\text{H}_{48}\text{B}_6\text{P}_3\text{Ce}$: H, 6.21%. Found: H, 6.18%. ^1H NMR (500 MHz, CD_2Cl_2): δ 6.69, 7.18, 7.36, 7.76, 8.64 (br s, Ph), 20.8 (br s, FWHM = 480 Hz, 12 H, BH_3 , dimer), 23.8 (br s, FWHM = 420 Hz, 18 H, BH_3 , monomer), 33.0 (br s, FWHM = 470 Hz, 6 H, BH_3 , dimer). ^{11}B NMR (160 MHz, CD_2Cl_2): δ 3.1 (br s, FWHM = 440 Hz, BH_3 , dimer), 11.4 (br s, FWHM = 370 Hz, BH_3 , monomer), 44.0 (br s, FWHM = 510 Hz, BH_3 , dimer). IR (KBr) $\bar{\nu}_{\text{max}}$ (cm^{-1}): 3144 (w), 3074 (w), 3057 (m), 3022 (w), 3005 (w), 2963 (w), 2438 (m, BH_3), 2413 (m,

BH₃), 2357 (m, BH₃), 2249 (s, BH₃), 1961 (w), 1885 (w), 1812 (w), 1762 (w), 1671 (w), 1617 (w), 1586 (w), 1572 (w), 1539 (w), 1482 (m), 1435 (s), 1384 (w), 1330 (w), 1307 (w), 1216 (s), 1183 (s), 1106 (w), 1084 (m), 1052 (s), 1027 (m), 999 (m), 921 (w), 848 (w), 781 (w), 738 (s), 703 (s), 691 (s), 623 (m), 612 (m).

Tris(diphenylphosphinodiboranato)praseodymium(III), Pr(H₃BPPPh₂BH₃)₃ (3). Prepared as described for **1** with PrI₃ (0.105 g, 0.201 mmol) and K(H₃BP'Bu₂BH₃) (0.145 g, 0.575 mmol). Yield: 105 mg (83%). Anal. Calcd. For C₃₆H₄₈B₆P₃Pr: H, 6.21%. Found: H, 5.96%. ¹H NMR (500 MHz, CD₂Cl₂): δ 5.85, 6.76, 6.88, 7.33, 7.61, 10.09 (br s, 70 H, Ph), 55.8 (br s, FWHM = 500 Hz, 12 H, BH₃, dimer), 63.8 (br s, FWHM = 550 Hz, 18 H, BH₃, monomer), 79.0 (br s, FWHM = 300 Hz, BH₃, dimer). ¹¹B NMR (160 MHz, CD₂Cl₂): δ 46.3 (br s, FWHM = 370 Hz, BH₃, dimer), 66.1 (br s, FWHM = 380 Hz, BH₃, monomer), 147.2 (br s, FWHM = 342 Hz, BH₃, dimer). IR (KBr) $\bar{\nu}_{\max}$ (cm⁻¹): 3074 (w), 3058 (w), 2921 (w), 2853 (w), 2436 (m), 2412 (m), 2244 (s), 2138 (w), 1982 (w), 1962 (w), 1886 (w), 1812 (w), 1761 (w), 1672 (w), 1586 (w), 1572 (w), 1482 (m), 1434 (s), 1384 (w), 1330 (w), 1307 (w), 1213 (s), 1183 (s), 1106 (s), 1080 (w), 1049 (s), 1027 (m), 999 (s), 921 (w), 865 (w), 844 (w), 782 (m), 746 (s), 701 (s), 690 (s), 622 (s), 612 (s).

Tris(diphenylphosphinodiboranato)neodymium(III), Nd(H₃BPPPh₂BH₃)₃ (4). Prepared as described for **1** with NdI₃ (0.102 g, 0.194 mmol) and K(H₃BP'Bu₂BH₃) (0.143 g, 0.568 mmol). Yield: 96.6 mg (77%). Anal. Calcd. For C₃₆H₄₈B₆P₃Nd: H, 6.18%. Found: H, 6.00%. ¹H NMR (400 MHz, CD₂Cl₂): δ 7.47, 7.73, 8.17 (br, 72 H, Ph), 77.3 (br s, FWHM = 550 Hz, 6 H, BH₃, dimer), 78.3 (br m, FWHM = 520 Hz, 18 H, BH₃, monomer), 83.5 (br s, FWHM = 510 Hz, 12 H, BH₃, dimer). ¹¹B NMR (128 MHz, CD₂Cl₂): δ 75.6 (br s, FWHM = 490 Hz, BH₃, dimer), 95.3 (br s, FWHM = 390 Hz, BH₃, monomer), 176.5 (br s, FWHM = 440 Hz, BH₃ dimer). IR (KBr) $\bar{\nu}_{\max}$ (cm⁻¹): 3074 (w), 3057 (w), 3021 (w), 3005 (w), 2986 (w), 2438 (m, BH₃), 2412 (m, BH₃), 2247 (m, BH₃) 1983 (w), 1961 (w), 1885 (w), 1812 (w), 1761 (w), 1671 (w), 1482 (w), 1435 (s), 1384 (w), 1330 (w), 1307 (w), 1221 (s), 1183 (s), 1107 (s), 1080 (m), 1050 (s), 999 (m), 9279 (w), 845 (w), 785 (m), 740 (m), 702 (s), 692 (s), 623 (m), 626 (m).

Tris(diphenylphosphinodiboranato)tris(tetrahydrofuran)neodymium(III), Nd(H₃BPPPh₂BH₃)₃(THF)₃ (4-THF). In a 2-dram vial, 0.050 g of **4** was dissolved in THF (ca. 1 mL). Vapor diffusion with Et₂O yielded small light purple blocks the next morning. Yield: 58 mg (67%). ¹H NMR (400 MHz, CD₂Cl₂): δ 4.59 (s, Ph), 5.54 and 7.48 (br s, Ph), 6.92 and 7.08 (br s, THF), 47.7 (br s, FWHM = 1100 Hz, BH₃), 50.7 (br s, FWHM = 1200 Hz, BH₃), 64.8 (br s, FWHM = 670 Hz, BH₃). ¹¹B NMR (128 MHz, CD₂Cl₂): δ 45.4 (br s, BH₃, FWHM = 820 Hz), 55.0 (br s, BH₃, FWHM = 660 Hz), 71.8 (br s, BH₃, FWHM = 470 Hz). IR (KBr) $\bar{\nu}_{\max}$ (cm⁻¹): 3073 (w), 3054 (m), 2978 (m), 2896 (m), 2428 (m, BH₃), 2358 (s, BH₃), 2331 (s, BH₃), 2259 (s, BH₃), 1962 (s), 1890 (s), 1816 (s), 1772 (s), 1673 (s), 1586 (s), 1572 (s), 1481 (m), 1457 (w), 1435 (s), 1386 (w), 1367 (w), 1346 (w), 1332 (w), 1308 (w), 1217 (m), 1182 (m), 1159 (w), 1132 (w), 1106 (m), 1059 (s), 1028 (m), 1003 (s, THF), 978 (w), 921 (m), 853 (m, THF), 736 (s), 702 (s), 694 (s), 669 (m), 618 (m).

Diido(phosphinodiboranato)tris(tetrahydrofuran)uranium(III), U(H₃BPH₂BH₃)₂(THF)₃ (5). U₂(THF)₄ (0.100 g, 0.111 mmol) and K(H₃BPH₂BH₃) (0.0331 g, 0.332 mmol) were loaded into a 5 mL FTS ball milling jar with two 5 mm stainless steel balls and several drops of Et₂O. The jar was hermetically sealed, placed on the FTS shaker mill, and milled for three hours. The jar was transferred into a glovebox and opened to reveal a dark red brown paste. The contents were

extracted with 20 mL of chlorobenzene, stirred to homogenize, then filtered over a fine frit. The residue was washed with copious amounts of chlorobenzene (ca. 60 mL) then stripped down to dryness to reveal a red oil. The oil was dissolved in the minimal amount of THF (ca. 1 mL), and vapor diffused with pentane to yield small red blocks the following day. Yield: 5.3 mg (6.2%). IR (ATR) $\bar{\nu}_{\text{max}}$ (cm⁻¹): 2989 (w), 2920 (m), 2853 (m), 2438 (m), 2401 (w), 2368 (m), 2240 (m), 1456 (w), 1436 (w), 1377 (w), 1365 (w), 1342 (w), 1294 (w), 1218 (m), 1177 (w), 1147 (w), 1058 (s, THF), 1004 (s, THF), 917 (w), 887 (m), 835 (s, THF), 666 (m).

XRD studies. Suitable crystals for single-crystal X-ray diffraction were grown from either DCM and Et₂O (**1a** and **1b**, **2**, **3**, and **4**), THF and Et₂O (**4-THF**), or THF and pentane (**5**) and mounted on a MiTeGen micromount with ParatoneN oil. Crystallographic data were collected using a Bruker Nonius Kappa ApexII, equipped with a charge-coupled-device (CCD) detector and cooled to 150 K using an Oxford Cryostreams 700 low temperature device or a Bruker D8 Venture Duo, equipped with a Bruker photon III detector and cooled to 150 K using an Oxford Cryostreams 800C low temperature device. Data were collected with MoK_α radiation ($\lambda = 0.71073 \text{ \AA}$). A hemisphere of data was collected using phi and omega scans. The data were corrected for absorption using redundant reflections and the SADABS program.⁹⁸ Structures were solved with intrinsic phasing (SHELXT) or direct methods (SHELXS) and least square refinement (SHELXL) confirmed the positions of all non-hydrogen atoms.⁹⁸ All hydrogen atom positions were idealized and were allowed to ride on the attached carbon and boron atoms. B-H bond distances were fixed at 1.2 Å. Structure solution and refinement were performed with Olex2.⁹⁹

Electronic Supplementary Information (ESI) available:

CCDC 2089074-2089078, 2089081, and 2089083. For ESI and crystallographic data in CIF format see DOI:

Acknowledgments

This material is based upon work supported by the U.S. Department of Energy (DOE), Office of Science, Office of Basic Energy Sciences, Separation Science program under Award DESC0019426. We thank Dale Swenson for collecting the single-crystal XRD data. T.V.F. would also like to thank Amy Charles for her assistance in the organization and revisions of this manuscript via the UIowa Chemistry reading and writing group. T.V.F. also gratefully acknowledges a post comprehensive exam fellowship from the University of Iowa Graduate College.

References

- (1) Fernandez-Bertran, J. F. *Pure Appl. Chem.* **1999**, *71*, 581-586.
- (2) Beyer, M. K.; Clausen-Schaumann, H. *Chem. Rev.* **2005**, *105*, 2921-2948.

- (3) Kaupp, G. *CrystEngComm* **2009**, *11*, 388-403.
- (4) James, S. L.; Adams, C. J.; Bolm, C.; Braga, D.; Collier, P.; Friscic, T.; Grepioni, F.; Harris, K. D. M.; Hyett, G.; Jones, W.; Krebs, A.; Mack, J.; Maini, L.; Orpen, A. G.; Parkin, I. P.; Shearouse, W. C.; Steed, J. W.; Waddell, D. C. *Chem. Soc. Rev.* **2012**, *41*, 413-447.
- (5) Boldyreva, E. *Chem. Soc. Rev.* **2013**, *42*, 7719-7738.
- (6) Takacs, L. *Chem. Soc. Rev.* **2013**, *42*, 7649-7659.
- (7) Jones, W.; Eddleston, M. D. *Faraday Discuss.* **2014**, *170*, 9-34.
- (8) Do, J.-L.; Friscic, T. *ACS Cent. Sci.* **2017**, *3*, 13-19.
- (9) Friscic, T.; Mottillo, C.; Titi, H. M. *Angew. Chem., Int. Ed.* **2020**, *59*, 1018-1029.
- (10) Fiss, B. G.; Richard, A. J.; Douglas, G.; Kojic, M.; Friscic, T.; Moores, A. *Chem. Soc. Rev.* **2021**, Ahead of Print.
- (11) Horie, K.; Barón, M.; Fox, R. B.; He, J.; Hess, M.; Kahovec, J.; Kitayama, T.; Kubisa, P.; Maréchal, E.; Mormann, W.; Stepto, R. F. T.; Tabak, D.; Vohlídal, J.; Wilks, E. S.; Work, W. J. *Pure and Applied Chemistry* **2004**, *76*, 889-906.
- (12) McNaught, A. D.; Wilkinson, A. *IUPAC Compendium of Chemical Terminology*; International Union of Pure and Applied Chemistry.
- (13) Garay, A. L.; Pichon, A.; James, S. L. *Chem. Soc. Rev.* **2007**, *36*, 846-855.
- (14) Wang, G.-W. *Chem. Soc. Rev.* **2013**, *42*, 7668-7700.
- (15) Hernandez, J. G.; Friscic, T. *Tetrahedron Lett.* **2015**, *56*, 4253-4265.
- (16) Rightmire, N. R.; Hanusa, T. P. *Dalton Trans.* **2016**, *45*, 2352-2362.
- (17) Hernandez, J. G.; Bolm, C. *J. Org. Chem.* **2017**, *82*, 4007-4019.
- (18) Geciauskaite, A. A.; Garcia, F. *Beilstein J. Org. Chem.* **2017**, *13*, 2068-2077.
- (19) Strukil, V. *Synlett* **2018**, *29*, 1281-1288.
- (20) Howard, J. L.; Cao, Q.; Browne, D. L. *Chem. Sci.* **2018**, *9*, 3080-3094.
- (21) Tan, D.; Friscic, T. *Eur. J. Org. Chem.* **2018**, *2018*, 18-33.
- (22) Beillard, A.; Bantreil, X.; Métro, T.-X.; Martinez, J.; Lamaty, F. *Chem. Rev.* **2019**, *119*, 7529-7609.
- (23) Bose, A.; Mal, P. *Beilstein J. Org. Chem.* **2019**, *15*, 881-900.
- (24) Tan, D.; Garcia, F. *Chem. Soc. Rev.* **2019**, *48*, 2274-2292.
- (25) Braga, D.; Giaffreda, S. L.; Grepioni, F.; Pettersen, A.; Maini, L.; Curzi, M.; Polito, M. *Dalton Trans.* **2006**, 1249-1263.

- (26) Balaz, P.; Achimovicova, M.; Balaz, M.; Billik, P.; Cherkezova-Zheleva, Z.; Criado, J. M.; Delogu, F.; Dutkova, E.; Gaffet, E.; Gotor, F. J.; Kumar, R.; Mitov, I.; Rojac, T.; Senna, M.; Streletskii, A.; Wieczorek-Ciurowa, K. *Chem. Soc. Rev.* **2013**, *42*, 7571-7637.
- (27) Xu, C.; De, S.; Balu, A. M.; Ojeda, M.; Luque, R. *Chem. Commun.* **2015**, *51*, 6698-6713.
- (28) Dreizin, E. L.; Schoenitz, M. *J. Mater. Sci.* **2017**, *52*, 11789-11809.
- (29) Zhang, P.; Dai, S. *J. Mater. Chem. A* **2017**, *5*, 16118-16127.
- (30) Miao, Y.-R.; Suslick, K. S. *Adv. Inorg. Chem.* **2018**, *71*, 403-434.
- (31) Munoz-Batista, M. J.; Rodriguez-Padron, D.; Puente-Santiago, A. R.; Luque, R. *ACS Sustainable Chem. Eng.* **2018**, *6*, 9530-9544.
- (32) Chen, D.; Zhao, J.; Zhang, P.; Dai, S. *Polyhedron* **2019**, *162*, 59-64.
- (33) Delori, A.; Friscic, T.; Jones, W. *CrystEngComm* **2012**, *14*, 2350-2362.
- (34) Perez-Venegas, M.; Juaristi, E. *ACS Sustainable Chem. Eng.* **2020**, *8*, 8881-8893.
- (35) Do, J.-L.; Friscic, T. *Synlett* **2017**, *28*, 2066-2092.
- (36) Ardila-Fierro, K. J.; Hernandez, J. G. *ChemSusChem* **2021**, *14*, 2145-2162.
- (37) Volkov, V. V.; Myakishev, K. G. *Inorg. Chim. Acta* **1999**, *289*, 51-57.
- (38) Mal'tseva, N. N.; Generalova, N. B.; Masanov, A. Y.; Zhizhin, K. Y.; Kuznetsov, N. T. *Russ. J. Inorg. Chem.* **2012**, *57*, 1631-1652.
- (39) Volkov, V. V.; Myakishev, K. G. *Radiokhimiya* **1976**, *18*, 512-513.
- (40) Huot, J.; Cuevas, F.; Deledda, S.; Edalati, K.; Filinchuk, Y.; Grosdidier, T.; Hauback, C. B.; Heere, M.; Jensen, R. T.; Latroche, M.; Sartori, S. *Materials* **2019**, *12*, 2778.
- (41) Paskevicius, M.; Jepsen, L. H.; Schouwink, P.; Cerny, R.; Ravnsbaek, D. B.; Filinchuk, Y.; Dornheim, M.; Besenbacher, F.; Jensen, T. R. *Chem. Soc. Rev.* **2017**, *46*, 1565-1634.
- (42) Daly, S. R.; Kim, D. Y.; Yang, Y.; Abelson, J. R.; Girolami, G. S. *J. Am. Chem. Soc.* **2010**, *132*, 2106-2107.
- (43) Daly, S. R.; Kim, D. Y.; Girolami, G. S. *Inorg. Chem.* **2012**, *51*, 7050-7065.
- (44) Rightmire, N. R.; Hanusa, T. P.; Rheingold, A. L. *Organometallics* **2014**, *33*, 5952-5955.
- (45) Woen, D. H.; Kotyk, C. M.; Mueller, T. J.; Ziller, J. W.; Evans, W. J. *Organometallics* **2017**, *36*, 4558-4563.
- (46) Woen, D. H.; White, J. R. K.; Ziller, J. W.; Evans, W. J. *J. Organomet. Chem.* **2019**, *899*, 120885.
- (47) Fetrow, T. V.; Bhowmick, R.; Achazi, A. J.; Blake, A. V.; Eckstrom, F. D.; Vlaisavljevich, B.; Daly, S. R. *Inorg. Chem.* **2020**, *59*, 48-61.

- (48) Blake, A. V.; Fetrow, T. V.; Theiler, Z. J.; Vlaisavljevich, B.; Daly, S. R. *Chem. Commun.* **2018**, *54*, 5602-5605.
- (49) Daly, S. R.; Piccoli, P. M. B.; Schultz, A. J.; Todorova, T. K.; Gagliardi, L.; Girolami, G. S. *Angew. Chem., Int. Ed.* **2010**, *49*, 3379-3381.
- (50) Daly, S. R.; Girolami, G. S. *Chem. Commun.* **2010**, *46*, 407-408.
- (51) Daly, S. R.; Girolami, G. S. *Inorg. Chem.* **2010**, *49*, 4578-4585.
- (52) Daly, S. R.; Girolami, G. S. *Inorg. Chem.* **2010**, *49*, 5157-5166.
- (53) Daly, S. R.; Bellott, B. J.; Kim, D. Y.; Girolami, G. S. *J. Am. Chem. Soc.* **2010**, *132*, 7254.
- (54) Chang, N. N.; Daly, S. R.; Girolami, G. S. *Polyhedron* **2019**, *162*, 52.
- (55) Zohari, N.; Fareghi-Alamdari, R.; Sheibani, N. *New J. Chem.* **2020**, *44*, 7436-7449.
- (56) Thompson, N. R. *J. Chem. Soc.* **1965**, 6290-6295.
- (57) Rudzevich, V. L.; Gornitzka, H.; Romanenko, V. D.; Bertrand, G. *Chem. Commun.* **2001**, 1634-1635.
- (58) Mayer, E.; Laubengayer, A. W. *Monatsh. Chem.* **1970**, *101*, 1138-1144.
- (59) Mayer, E.; Hester, R. E. *Spectrochim. Acta, Part A* **1969**, *25*, 237-243.
- (60) Mayer, E. *Angew. Chem., Int. Ed.* **1971**, *10*, 416-417.
- (61) Majhi, P. K.; Koner, A.; Schnakenburg, G.; Kelemen, Z.; Nyulaszi, L.; Streubel, R. *Eur. J. Inorg. Chem.* **2016**, *2016*, 3559-3573.
- (62) Keller, P. C.; Schwartz, L. D. *Inorg. Chem.* **1971**, *10*, 645-647.
- (63) Izod, K.; Watson, J. M.; Harrington, R. W.; Clegg, W. *Dalton Trans.* **2021**, *50*, 1019-1024.
- (64) Izod, K.; Watson, J. M.; Clegg, W.; Harrington, R. W. *Inorg. Chem.* **2013**, *52*, 1466-1475.
- (65) Izod, K.; Watson, J. M.; Clegg, W.; Harrington, R. W. *Dalton Trans.* **2011**, *40*, 11712-11718.
- (66) Hooper, T. N.; Huertos, M. A.; Jurca, T.; Pike, S. D.; Weller, A. S.; Manners, I. *Inorg. Chem.* **2014**, *53*, 3716-3729.
- (67) Hofstoetter, H.; Mayer, E. *Monatsh. Chem.* **1974**, *105*, 712-725.
- (68) Hofstoetter, H.; Mayer, E. *Angew. Chem.* **1973**, *85*, 410-411.
- (69) Hester, R. E.; Mayer, E. *Spectrochim. Acta, Part A* **1967**, *23*, 2218-2220.
- (70) Girolami, G. S.; Kim, D. Y.; Abelson, J. R.; Kumar, N.; Yang, Y.; Daly, S.; The Board of Trustees of the University of Illinois, USA . 2013, p No pp. given.
- (71) Gilje, J. W.; Morse, K. W.; Parry, R. W. *Inorg. Chem.* **1967**, *6*, 1761-1765.
- (72) Fritz, G.; Pfannerer, F. *Z. Anorg. Allg. Chem.* **1970**, *373*, 30-35.

- (73) Dornhaus, F.; Bolte, M.; Lerner, H.-W.; Wagner, M. *Eur. J. Inorg. Chem.* **2006**, 1777-1785.
- (74) Cordaro, J. G.; Sandia Corporation, USA . 2013, p 7.
- (75) Centofanti, L. F. *Inorg. Chem.* **1973**, *12*, 1131-1133.
- (76) Bhattacharyya, K. X.; Dreyfuss, S.; Saffon-Merceron, N.; Mezailles, N. *Chem. Commun.* **2016**, *52*, 5179-5182.
- (77) Anstey, M. R.; Corbett, M. T.; Majzoub, E. H.; Cordaro, J. G. *Inorg. Chem.* **2010**, *49*, 8197-8199.
- (78) Maser, L.; Flosdorf, K.; Langer, R. *J. Organomet. Chem.* **2015**, *791*, 6-12.
- (79) Morris, L. J.; Hill, M. S.; Mahon, M. F.; Manners, I.; Patrick, B. O. *Organometallics* **2020**, *39*, 4195-4207.
- (80) Dornhaus, F.; Bolte, M. *Acta Crystallogr., Sect. E: Struct. Rep. Online* **2006**, *62*, m3573-m3575.
- (81) Zhang, W.; Qi, X.; Huang, S.; Li, J.; Tang, C.; Li, J.; Zhang, Q. *Journal of Materials Chemistry A* **2016**, *4*, 8978-8982.
- (82) Bowmaker, G. A. *Chem. Commun.* **2013**, *49*, 334-348.
- (83) Gompa, T. P.; Rice, N. T.; Russo, D. R.; Aguirre Quintana, L. M.; Yik, B. J.; Bacsa, J.; La Pierre, H. S. *Dalton Trans.* **2019**, *48*, 8030-8033.
- (84) Shinomoto, R.; Gamp, E.; Edelstein, N. M.; Templeton, D. H.; Zalkin, A. *Inorg. Chem.* **1983**, *22*, 2351-2355.
- (85) Shannon, R. D. *Acta Crystallogr., Sect. A: Cryst. Phys., Diffr., Theor. Gen. Crystallogr.* **1976**, *A32*, 751.
- (86) Marks, T. J.; Kolb, J. R. *Chem. Rev.* **1977**, *77*, 263-293.
- (87) Daly, S. R. In *The Heaviest Metals: Science and Technology of the Actinides and Beyond*; Evans, W. J., Hanusa, T. P., Eds. 2018, p 319.
- (88) Braunschweig, H.; Gackstatter, A.; Kupfer, T.; Radacki, K.; Franke, S.; Meyer, K.; Fucke, K.; Lemee-Cailleau, M. H. *Inorg. Chem.* **2015**, *54*, 8022-8028.
- (89) Bernstein, E. R.; Hamilton, W. C.; Keiderling, T. A.; La Placa, S. J.; Lippard, S. J.; Mayerle, J. J. *Inorg. Chem.* **1972**, *11*, 3009-3016.
- (90) Bernstein, E. R.; Keiderling, T. A.; Lippard, S. J.; Mayerle, J. J. *J. Am. Chem. Soc.* **1972**, *94*, 2552-2553.

- (91) Schlesinger, H. I.; Brown, H. C. *Journal of the American Chemical Society* **1953**, *75*, 219-221.
- (92) Bochkarev, M. N. *Russ. Chem. Rev.* **2000**, *69*, 783-794.
- (93) Bochkarev, M. N. *Chem. Rev.* **2002**, *102*, 2089-2117.
- (94) Baudry, D.; Bulot, E.; Ephritikhine, M. *J. Chem. Soc., Chem. Commun.* **1988**, 1369-1370.
- (95) Baudry, D.; Bulot, E.; Charpin, P.; Ephritikhine, M.; Lance, M.; Nierlich, M.; Vigner, J. *J. Organomet. Chem.* **1989**, *371*, 155-162.
- (96) Monreal, M. J.; Thomson, R. K.; Cantat, T.; Travia, N. E.; Scott, B. L.; Kiplinger, J. L. *Organometallics* **2011**, *30*, 2031-2038.
- (97) Fetrow, T. V.; Grabow, J. P.; Leddy, J.; Daly, S. R. *Inorg. Chem.* **2021**, *60*, 7593-7601.
- (98) Sheldrick, G. M. *Acta Crystallogr., Sect. A: Found. Crystallogr.* **2008**, *64*, 112.
- (99) Dolomanov, O. V.; Bourhis, L. J.; Gildea, R. J.; Howard, J. A. K.; Puschmann, H. *Journal of Applied Crystallography* **2009**, *42*, 339-341.